Validation of Satellite AIRS LST/LSE Products Using Aircraft Observations

Robert O. Knuteson, Brian J. Osborne, Henry E. Revercomb, and David C. Tobin
University of Wisconsin Space Science and Engineering Center, Madison, WI, USA

William L. Smith, Sr.
NASA Langley Research Center, Hampton, VA, USA

Introduction

Weather satellites have shown positive impact on forecast models for data collected over the world's oceans. However, the use of weather satellite data over land areas has been limited. One of the problems faced by users of broadband infrared measurements is the inability to separate the effect of land surface temperature (LST) from natural variations in land surface emissivity (LSE). A new generation of infrared sounders has been developed for obtaining improved profiles of atmospheric temperature, water vapor, and trace gas concentrations. A characteristic of these advanced sounders is the use of spectrometers with nearly continuous coverage of the 8-14 micron infrared window region with resolving powers of 1000 or greater. These high spectral resolution sounders have the advantage of being able to resolve individual absorption lines of water vapor and carbon dioxide and thereby provide a number of transparent "microwindows" that require a smaller atmospheric correction than broad-band instruments. In addition, it has been recognized that high spectral resolution infrared observations have another important advantage over broad band measurements in that they allow an effective surface temperature to be determined simultaneously with an effective land surface emissivity. A method for emissivity – temperature separation using high spectral resolution infrared observations has been developed at the University of Wisconsin Space Science and Engineering Center (UW-SSEC) in conjunction with NASA Langley Research Center (LaRC). The algorithm has been applied to UW-SSEC's ground-based Surface-Atmospheric Emitted Radiance Interferometer (S-AERI), the UW-SSEC Scanning High-resolution Interferometer Sounder (S-HIS) aircraft instrument, and the NPOESS Atmospheric Sounder Testbed – Interferometer (NAST-I) operated by NASA LaRC. Recently data from the NASA Atmospheric InfraRed Sounder (AIRS) satellite instrument have been compared with measurements from these ground-based and high altitude aircraft over the U.S. Department of Energy Atmospheric Radiation Measurement (ARM) Southern Great Plains (SGP) site in north central Oklahoma, USA. The lessons learned from this analysis have implications for the future operational use of data from the NPOESS CrIS and the METOP IASI sensors.

This paper includes the results of a ground-based survey of the validation site, results of a simulation of top of atmosphere upwelling infrared radiance observations at high spectral resolution, analysis of aircraft observations over the ground site, and comparison with results derived from the AIRS satellite instrument.

ARM Site Survey

The UW-SSEC conducted a ground-based survey of the DOE ARM SGP site in north central Oklahoma (USA) over a period of several years (1996-2003). This survey includes both a characterization of the land cover/land use in the vicinity of the ARM SGP central facility and

detailed measurements of the surface emissivity of selected land types. One of the co-authors developed the methodology shown in Figure 1 for the classification of the land cover (Osborne et al. 2003). The upper panel shows the 8x8 mile grid used in the ground-based survey of land cover while the lower pie chart shows the percentage occurrence of each class. The land cover is a mixture of permanent grassland pasture intermixed with fields of winter wheat and/or bare soil. The density of the wheat grass in each field leads to a change in the vegetation fraction during the growing season (from 0 to 100%). Figure 2 presents the results of the ground-based surface emissivity survey with the UW-SSEC S-AERI instrument (Knuteson et al. 2003). The key result from the emissivity survey is that the wheat field measurements can be represented as a linear combination of measurements of "pure" scene types; vegetation (grass) and bare soil (quartz mineral).

Simulated High Altitude Observations

This paper will follow the theory outlined in Knuteson et al. (2004). The cloud-free radiative transfer equation, neglecting solar radiation and scattering effects, for a downlooking infrared sensor viewing a homogeneous surface is given by the following equation

$$I_\nu = \int_0^Z B_\nu[T(z)]\frac{\partial \tau_\nu(z,Z)}{\partial z}\,dz + \varepsilon_\nu \cdot B_\nu(T_S) \cdot \tau_\nu(0,Z) + (1-\varepsilon_\nu) \cdot \tau_\nu(0,Z)\int_\infty^0 B_\nu[T(z)]\frac{\partial \tau_\nu(z,Z)}{\partial z}\,dz,$$

where I_ν, ε_ν, B_ν, T_s, $\tau_\nu(z_1,z_2)$, Z, and $T(z)$ are observed spectral radiance, spectral emissivity, spectral Planck function, the surface temperature, spectral transmittance at wavenumber ν from altitude z_1 to z_2, sensor altitude, and air temperature at altitude z, respectively. The first term of the equation is the emission from the atmosphere above the surface, the second term is the direct emission from the surface that reaches the sensor, and the third term is the downwelling atmospheric emission reflected off the ground under the approximation of a lambertian surface. The emissivity can be formally expressed (below) where R^{OBS} is the observed upwelling radiance,

$$\hat{\varepsilon}_\nu = \frac{[R_\nu^{OBS} - N_\nu^\uparrow] - \tau_\nu \overline{N}_\nu^\downarrow}{\tau_\nu B_\nu(\hat{T}_S) - \tau_\nu \overline{N}_\nu^\downarrow}$$

$$\frac{de_\nu}{e_\nu} = \frac{-B_\nu(T_S)}{B_\nu(T_S) - \overline{N}_\nu^\downarrow} \cdot \frac{dB_\nu(T_S)}{B_\nu(T_S)}$$

N^{UP} represents the upwelling emission from the atmosphere only and N^{DN} represents the downwelling flux at the surface. The ^ symbol denotes "effective" quantities as defined in Knuteson et al. (2004). The fractional change in emissivity is shown to vary on and off of spectral emission lines according to the reflected infrared radiance.

Figure 3 shows the result of a simulation of upwelling infrared radiance at 20 km altitude for the spectral resolution of the S-HIS instrument (0.5 cm^{-1} unapodized). The atmospheric pressure, temperature and water vapor are obtained from the combination of a Vaisala RS80H radiosonde, a Radiometrics microwave radiometer, and the CART Raman Lidar (CRL). The magnitude of the reflected contribution to the upwelling radiance is shown for each of three surface emissivity assumptions. Figure 4 illustrates the technique for the determination of the effective surface temperature by the minimization of the spectral variance in the derived surface emissivity spectrum. This "optimum" surface temperature is then used to compute the final derived effective emissivity spectrum. This technique is used for ground-based data where both the up and down welling radiance are measured, but it has also been successfully applied to aircraft and satellite measurements where the atmospheric contributions have been calculated using a line-by-line radiative transfer program.

Scanning-HIS and AIRS Results

Prior to the launch of the Aqua platform with the NASA AIRS instrument, the UW-SSEC conducted several aircraft campaigns to characterize the surface emissivity and surface temperature variations in the vicinity of the ARM SGP central facility at the spatial scales needed for validation of satellite products. Figure 5 illustrates the spatial scale of the Scanning HIS field of view (2 km) compared with that of AIRS (about 15 km). Observations from a NASA ER-2 flight of 31 March 2001 were analyzed by averaging the S-HIS footprints over a spatial dimension similar to that expected from the AIRS instrument. The result of the analysis directly over the ARM SGP central facility shows that the effective emissivity derived from the spatially averaged S-HIS data can be approximately represented as a linear combination of the pure scene types measured in the ground-based survey. A case study over the same validation site has been analyzed with AIRS satellite data collected on 16 November 2002. The broader spatial coverage of the satellite data is illustrated in Figure 6, which shows the observed brightness temperature at 12 μm over north central Oklahoma and southern Kansas. The symbols mark the central facility (diamond) and the boundary facilities (triangles). After application of the "online/offline" technique the distribution of surface temperature and emissivity assumes a very reasonable pattern. The cooler temperatures are associated with the high emissivity vegetation corresponding to the permanent grassland in the southeastern corner of the domain. The warmer (daytime) temperatures correspond to the "wheat belt" where at this time of year more of the bare soil is exposed. The central facility is in the wheat-growing zone but quite near the transition region. Figure 7 highlights some of the emissivity spectra derived from AIRS radiance observations near the ARM SGP central facility.

Conclusions

The high spectral resolution structure of the infrared surface reflection can be used to determine the effective value of Ts for which ε_v is constant across spectral absorption/emission lines. Using ground-based measurements at the ARM SGP site, area averaged emissivity can be accurately represented using a single parameter (vegetation fraction) and two pure scene types; vegetation (grass) and bare soil (quartz signature). The results of ground-based, aircraft-based, and satellite-based infrared observations are shown to provide a consistent representation of the surface emissivity in the vicinity of the ARM Southern Great Plains site. These research products will be used in the validation of the AIRS "standard" land surface products.

Acknowledgements

References

Knuteson, R. O., F. A. Best, D. H. DeSlover, B. J. Osborne, H. E. Revercomb, W. L. Smith, Sr., 2004: Infrared land surface remote sensing using high spectral resolution aircraft observations, *Adv. Space Res.*, Vol. 33, 2004 (in press).

Knuteson, R. O., R. G. Dedecker, W. F. Feltz, B. J. Osborne, H. E. Revercomb, D. C. Tobin, 2003: Infrared Land Surface Emissivity in the Vicinity of the ARM SGP Central Facility, Proc. of the Thirteenth ARM Science Team Meeting, Broomfield, CO, March 31–April 4, 2003.

Osborne, B. J., R. O. Knuteson, H. E. Revercomb, J. F. Short, and D. C. Tobin, 2003: Ground truth measurements for validation of AIRS land surface temperature and emissivity products at the Southern Great Plains validation site, in Fourier Transform Spectroscopy, OSA Technical Digest (Optical Society of America, Washington DC, 2003), Quebec City, 3–6 February 2003.
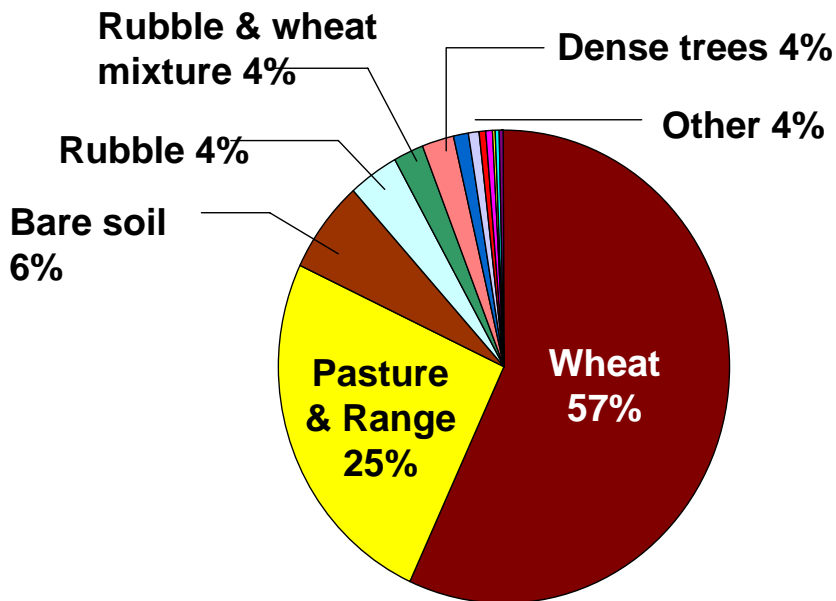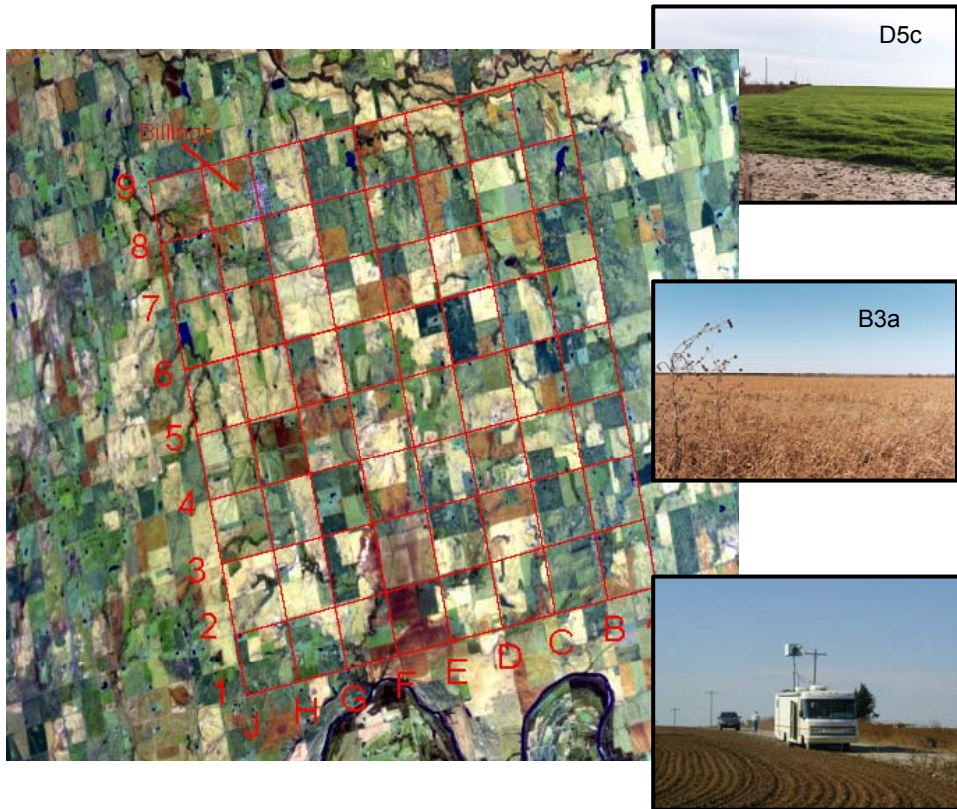
Fig. 1: The upper panel shows the 8x8 mile grid used in the ground-based survey of land cover in the vicinity of the DOE ARM SGP central facility. Land cover surveys were conducted by UW personnel in 2001, 2002, and 2003 at different times of the year. The results of the November 2002 survey are shown in the pie chart. The category "Pasture and Range" is composed of permanent grassland while the "Wheat" category is a mixture of wheat grass and bare soil which changes fraction during the growing season.
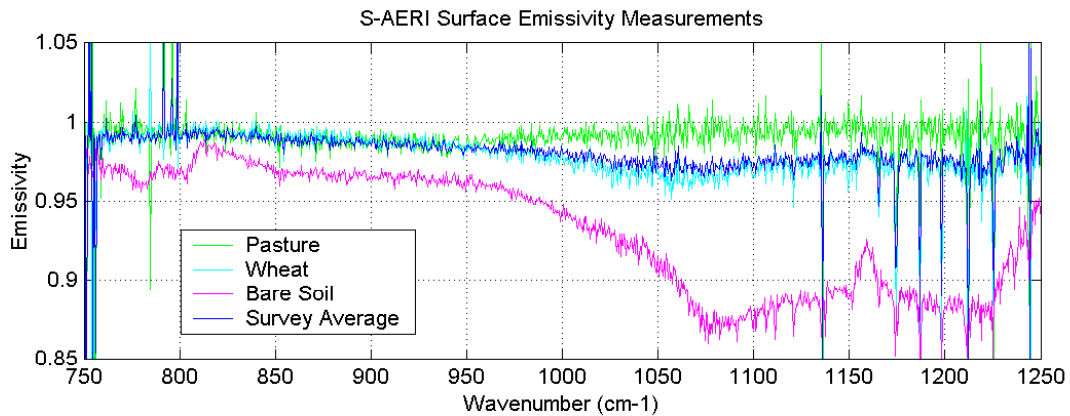
Fig. 2: UW ground-based emissivity survey conducted at the DOE ARM SGP central facility. The upper left photo shows a farm field in the early stages of winter wheat growth (March 2001). Notice the bare soil is visible between the small wheat plants at this time of year. The Scanning AERI, shown in the upper right, was used to measure the emissivities shown in the lower panel. The curve indicated as "wheat" in the plot is the measurement from the field shown above. The importance of this measurement is that the wheat measurement is very similar to the linear combination of "pure" scene types (grassland pasture and bare soil) obtained by the land cover survey. This suggests that the primary variable that determines the spectral contrast in surface emissivity is the fraction of vegetation in the instrument field of view. This result is true at all scales from the half meter scale of the ground-based Scanning AERI, to the 2 km scale of the Scanning HIS aircraft instrument, and the 15 km scale of the AIRS satellite instrument.
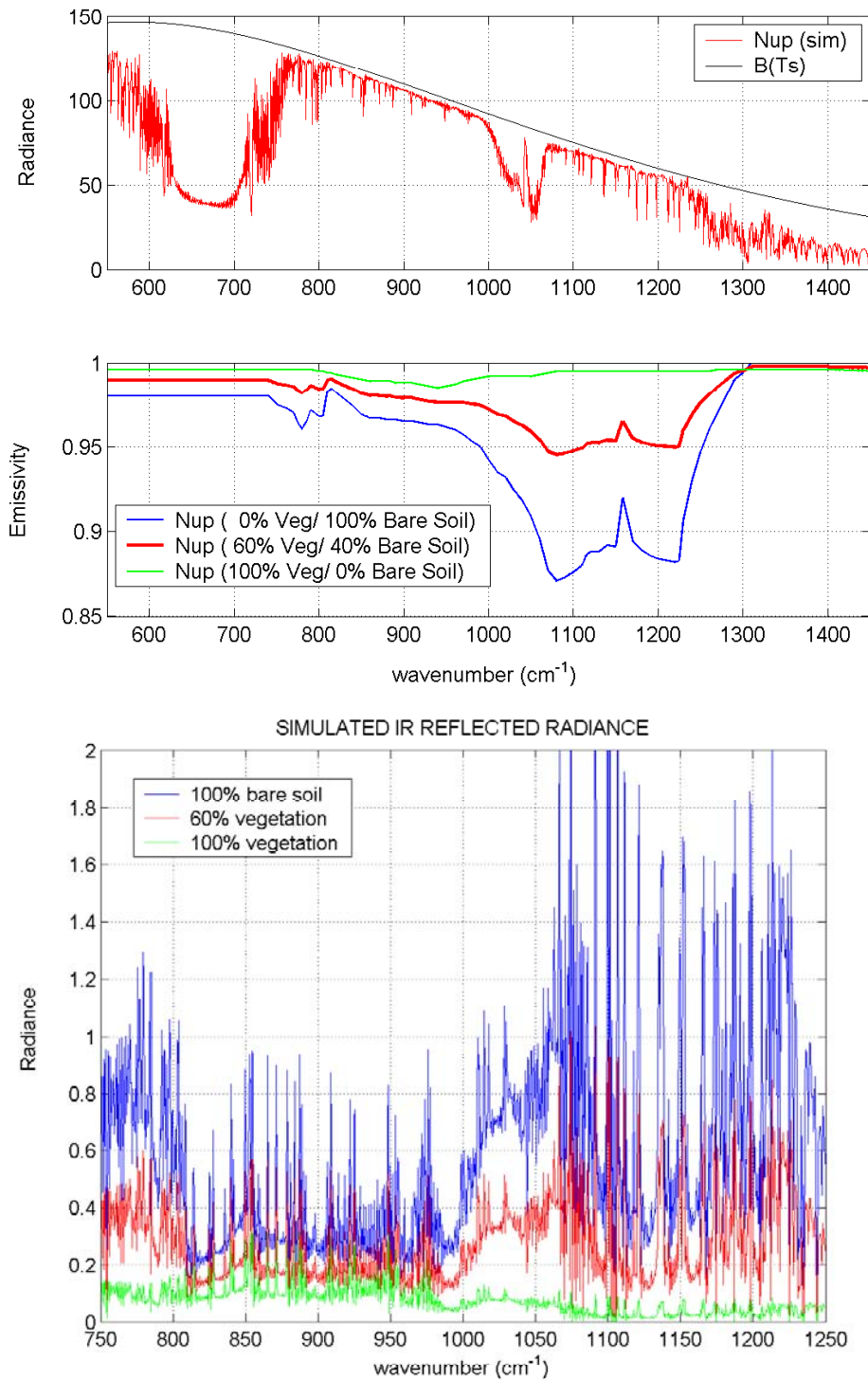
Fig. 3: Simulation of upwelling radiance at high spectral resolution (0.5 cm^{-1}) for an observer at 20 km (upper panel). This simulation uses the emissivity of pure scene types measured in the vicinity of the DOE ARM SGP central facility site and a linear combination suggested by the ground based survey (center panel). The lower panel shows the size of the infrared reflected radiance for each of the three emissivity curves.
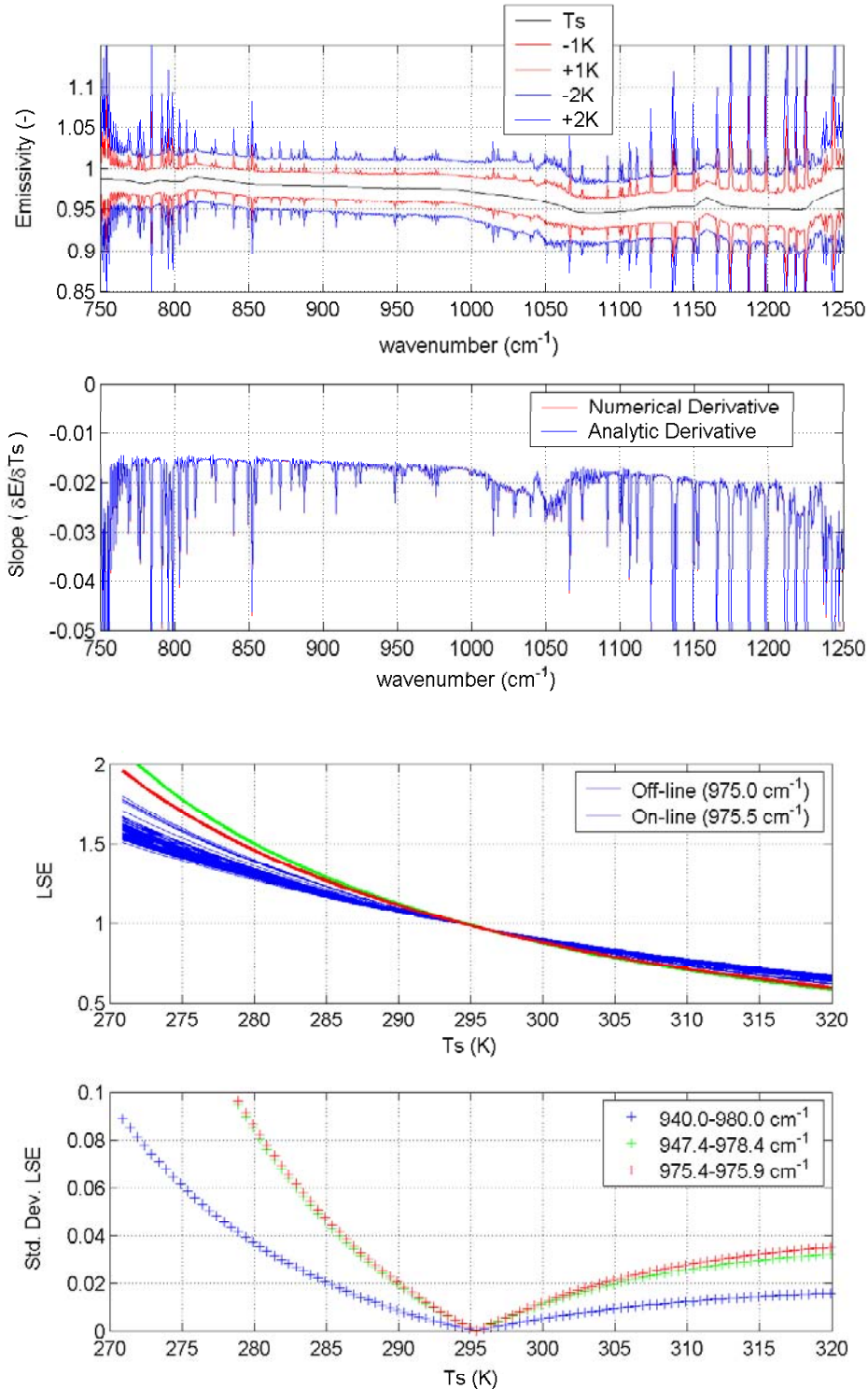
Fig. 4: Simulation of the derived emissivity as a function of land surface temperature. The top panel is the derived emissivity versus wavenumber for a range of surface temperatures. The second panel is the ratio of the change in emissivity for a change in surface temperature. The third panel shows on-line (red & green) versus off-line (blue) channels. The lower curve shows the true surface temperature is the minimum of the wavenumber standard deviation of emissivity as a function of surface temperature.
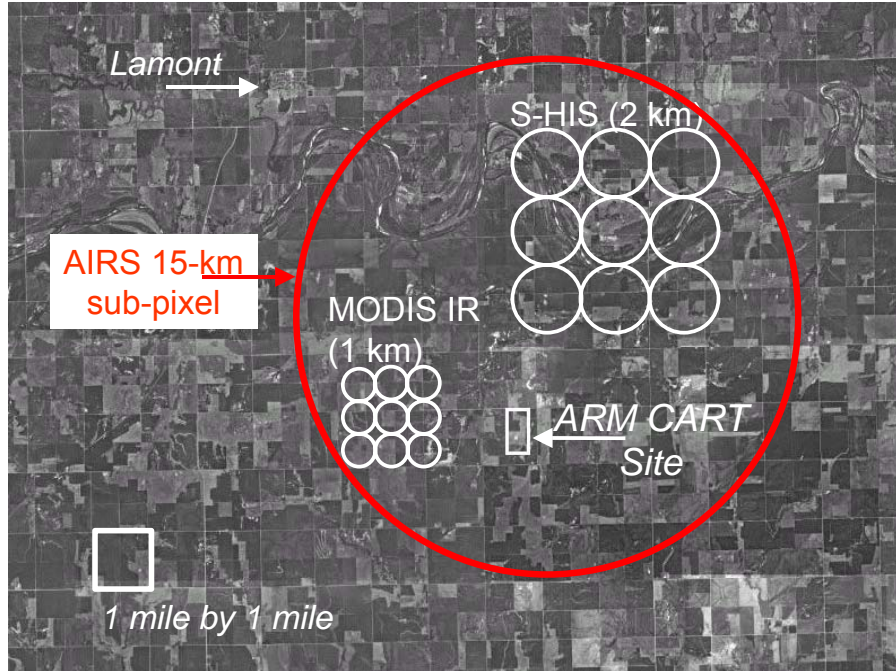
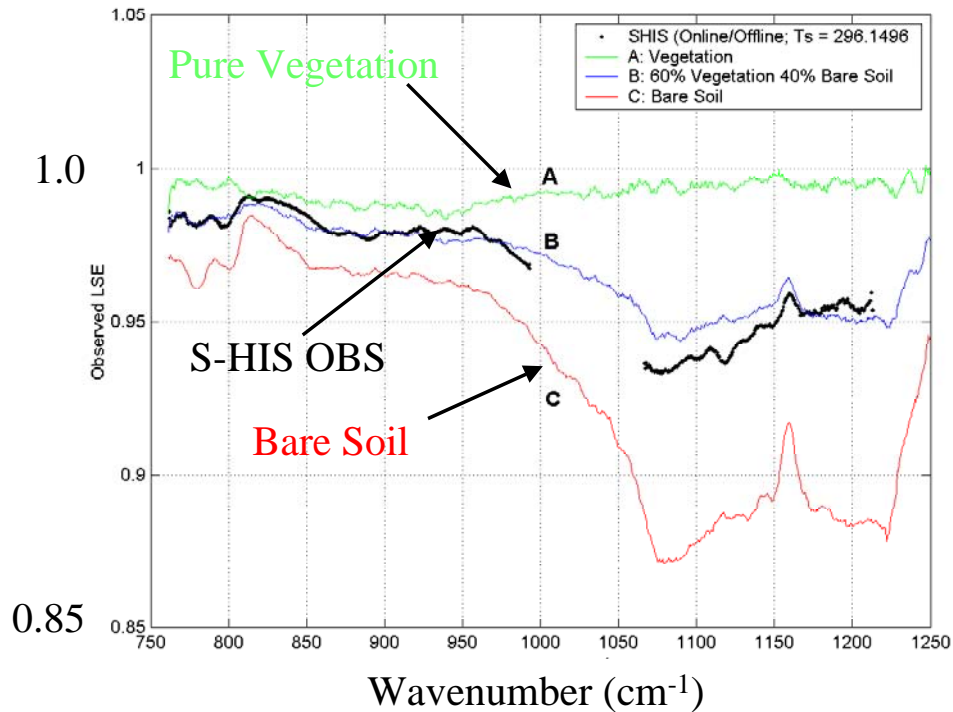*Aerial photo from http://terraserver.homeadvisor.msn.com/*

Fig. 5: The upper panel shows the approximate field of view sizes of AIRS, Scanning HIS, and MODIS instruments over an aerial photograph of the vicinity of the DOE ARM SGP central facility site. The lower panel shows that the effective land surface emissivity derived from Scanning HIS observations from 31 March 2001 18:45 UTC (averaged over 15 km) can be approximated by a linear combination of pure scene types (grass and bare soil). The best fit to these observations is 60% vegetation and 40% bare soil.
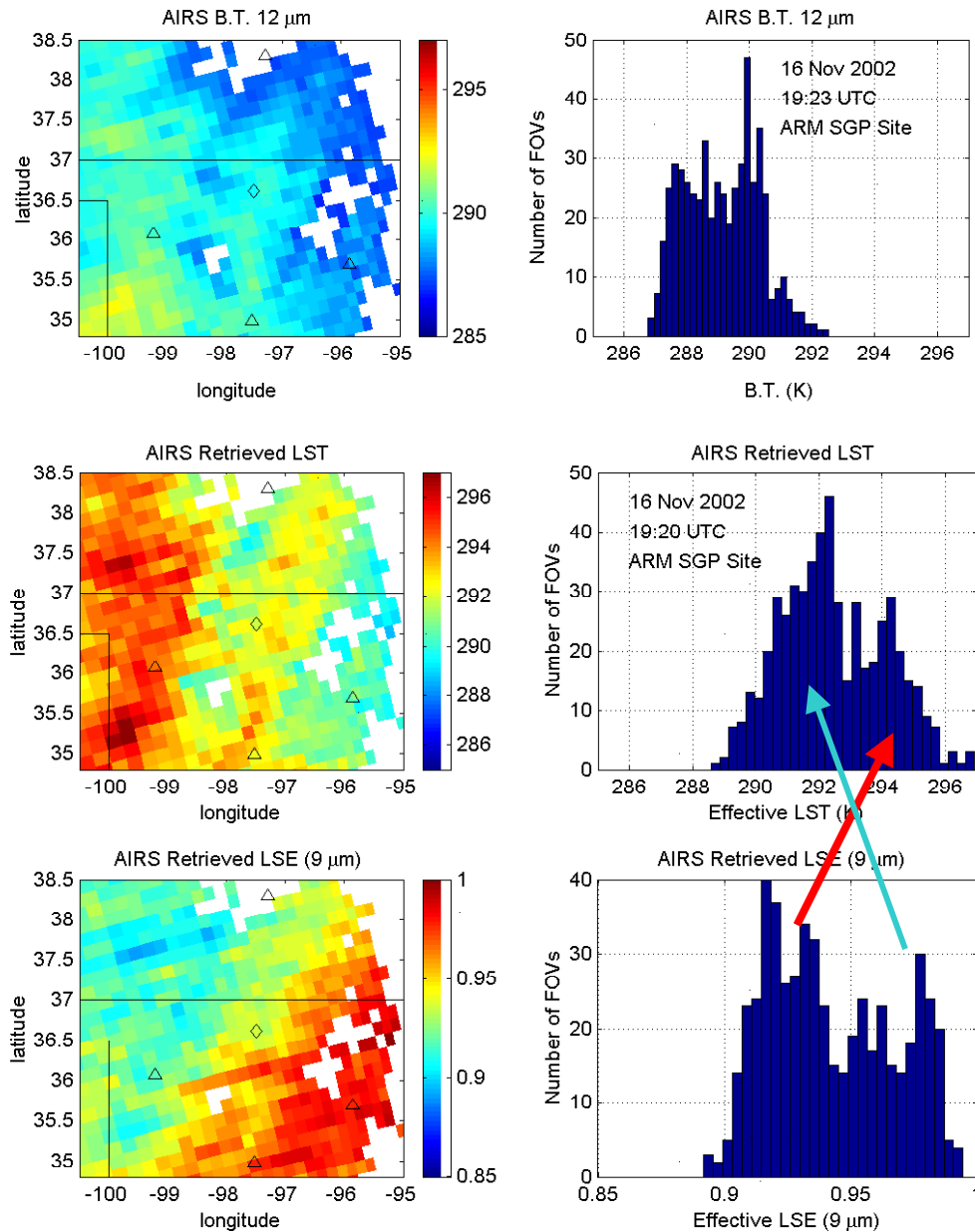
Fig. 6: The observed AIRS brightness temperature at 12 μm over the DOE ARM SGP site in north central Oklahoma, USA (16 Nov 2002 19 UTC) is shown in the upper panels as a brightness temperature map and as the corresponding histogram. The center panels show the land surface emissivity derived from the AIRS observations using the methodology described in the text. Note that the single brightness temperature distribution shifts to warmer temperatures and becomes two distinct distributions. The effective land surface emissivity derived simultaneously with the land surface temperature is shown in the lower panels. Lower emissivity values (at 9 μm) correspond to regions of higher surface temperaure. The results are consistent with the land cover survey which indicates that the central facility (indicated by the diamond symbol) is near the transition between high emissivity grassland (100% vegetation) to the southeast and wheat farming (mixed vegetation) with more low emissivity bare soil exposed.
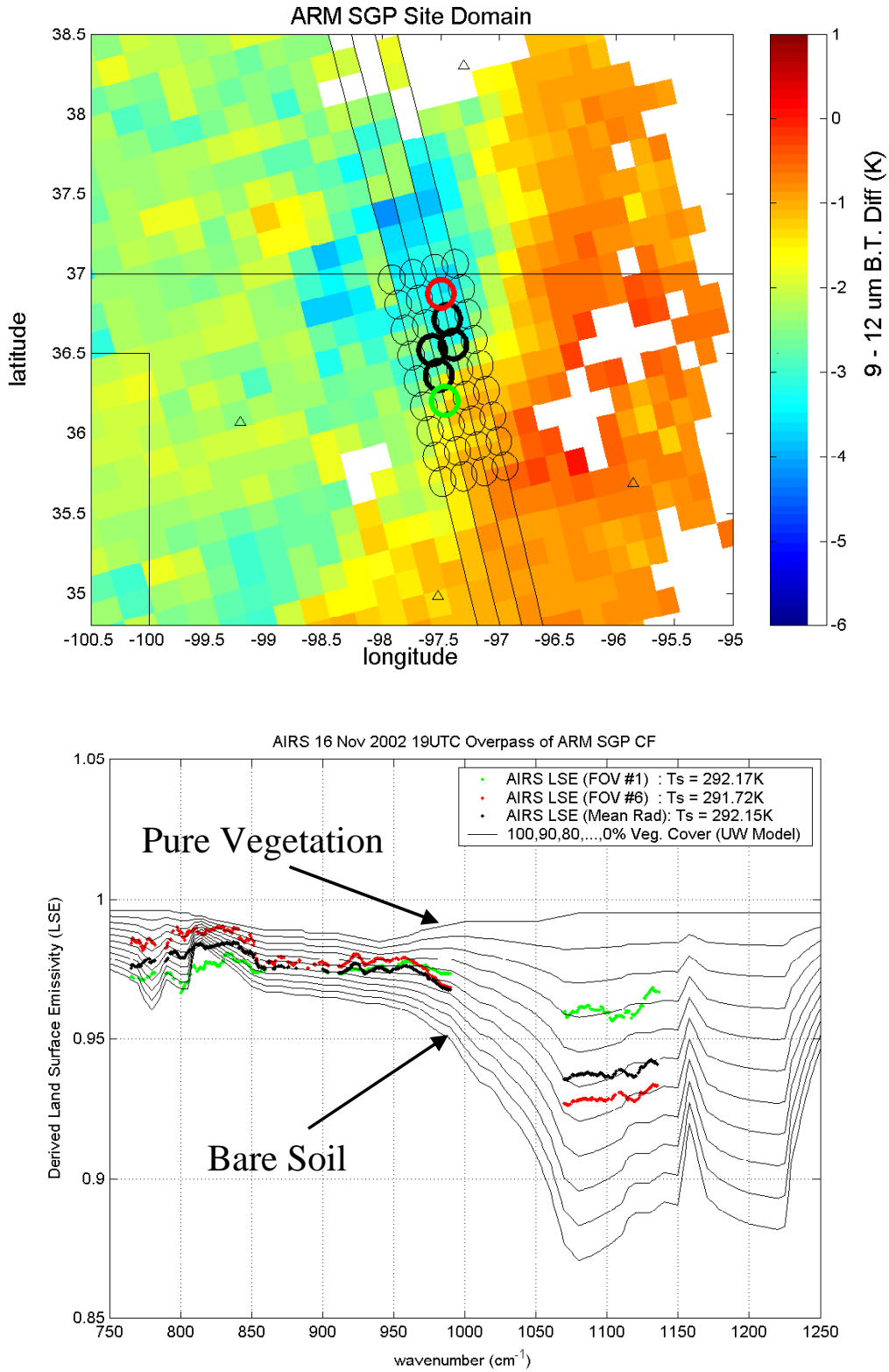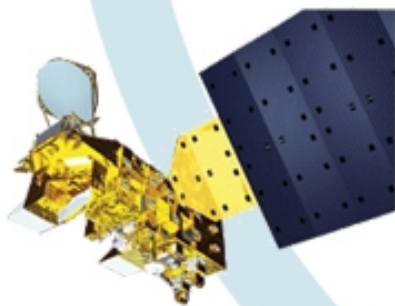
Fig. 7: Highlighted AIRS fields of view in the region near the DOE ARM SGP central facility (upper panel) show considerable variability in the effective emissivity (lower panel) derived from the AIRS radiances (16 Nov 2002 19 UTC). [UW Research Product]

Proceedings
of the
Thirteenth International
TOVS Study Conference

INTERNATIONAL
ATOVS
WORKING GROUP

Sainte-Adèle, Québec, Canada
29 October – 4 November 2003